

Title	Hole-injection barrier in pentacene field-effect transistor with Au electrodes modified by C ₁₆ H ₃₃ SH
Author(s)	Kawasaki, Naoko; Ohta, Yohei; Kubozono, Yoshihiro; Fujiwara, Akihiko
Citation	Applied Physics Letters, 91(12): 123518-1-123518-3
Issue Date	2007-09
Type	Journal Article
Text version	publisher
URL	http://hdl.handle.net/10119/3993
Rights	Copyright 2007 American Institute of Physics. This article may be downloaded for personal use only. Any other use requires prior permission of the author and the American Institute of Physics. The following article appeared in N. Kawasaki, Y. Ohta, Y. Kubozono, and A. Fujiwara, Applied Physics Letters 91(12), 123518 (2007) and may be found at http://link.aip.org/link/?apl/91/123518 .
Description	

Hole-injection barrier in pentacene field-effect transistor with Au electrodes modified by $C_{16}H_{33}SH$

Naoko Kawasaki, Yohei Ohta, and Yoshihiro Kubozono^{a)}

Research Laboratory for Surface Science, Okayama University, Okayama 700-8530, Japan

Akihiko Fujiwara

Japan Advanced Institute of Science and Technology, Ishikawa 923-1292, Japan

(Received 21 July 2007; accepted 4 September 2007; published online 21 September 2007)

Field-effect transistor with thin films of pentacene has been fabricated with Au electrodes modified by 1-hexadecanethiol ($C_{16}H_{33}SH$), and the hole-injection barriers have been determined from the temperature dependence of output properties on the basis of the thermionic emission model for double Schottky barriers. The large tunneling barriers are formed by the insulating $C_{16}H_{33}SH$ at the interfaces between the Au electrodes and pentacene thin films. © 2007 American Institute of Physics. [DOI: 10.1063/1.2789699]

Interface control is a very important technique for the realization of high-performance field-effect transistor (FET) devices. Recently, the Fermi level matching of the source/drain electrodes to the conduction/valence band of organic active layers produced *n*-, *p*-, and ambipolar FET properties.¹⁻³ These results opened the possibility of the FET devices with organic molecules. We also observed high μ value of $0.5 \text{ cm}^2 \text{ V}^{-1} \text{ s}^{-1}$ in the C_{60} FET with the Eu electrodes which possess low work function ϕ of 2.5 eV.⁴ This contact material has produced the Ohmic contact or effective carrier injection between the electrodes and C_{60} thin films.

In order to clarify the mechanism of carrier injection from electrodes to active layers, we analyzed the transport properties of the C_{60} FET devices with Au electrodes modified by 1-alkanethiols ($C_nH_{2n+1}SH$) on the basis of the thermionic emission model for double Schottky barriers.^{5,6} The effective Schottky barrier height ϕ_B^{eff} and tunneling efficiency β of electron for alkyl chains were determined and the electronic structures at the interface between the electrodes and C_{60} thin films were fully investigated. The ϕ_B^{eff} contains contributions from both Schottky barrier of pure Au- C_{60} junction and additional tunneling barrier formed by $C_nH_{2n+1}SH$. However, the Schottky barrier and the tunneling of the hole through alkyl chains at the interface of the *p*-channel organic FET devices have not been investigated so far.

In this study, we have investigated hole injection from the Au electrodes to pentacene thin films within the framework of thermionic emission model for double Schottky barriers.^{5,6} The pentacene thin-film FET device with Au electrodes modified by 1-hexadecanethiol ($C_{16}H_{33}SH$), pentacene/ $C_{16}H_{33}SH$ FET, showed large effective hole-injection barrier $\phi_{\text{bh}}^{\text{eff}}$ and it allowed us to provide useful information on Au-pentacene junctions in the FET device.

The device structure is shown in Fig. 1(a); the details of the dimensions are shown in the caption of Fig. 1(a). The processes for a cleaning of the surface of Si(100)/ SiO_2 wafers and for the formation of Au electrodes are described elsewhere.^{5,6} The surface of Au electrodes was modified with $C_{16}H_{33}SH$ by immersing the Si/ SiO_2 /Cr/Au substrates into the ethanol (EtOH) solution of $C_{16}H_{33}SH$ ($10^{-1} \text{ mol l}^{-1}$) for

47 h. The molecular structure of $C_{16}H_{33}SH$ is shown in Fig. 1(b). The substrates were washed with EtOH and ultrapure H_2O . The expected structure of $C_{16}H_{33}SH$ on the Au surface^{7,8} is shown in Fig. 1(c). The thin films (50 nm) of pentacene were formed on the substrate maintained at room temperature T by a thermal deposition under vacuum of 10^{-8} Torr. The transport characteristics of the FET devices were measured under vacuum of 10^{-6} Torr without annealing of the devices.

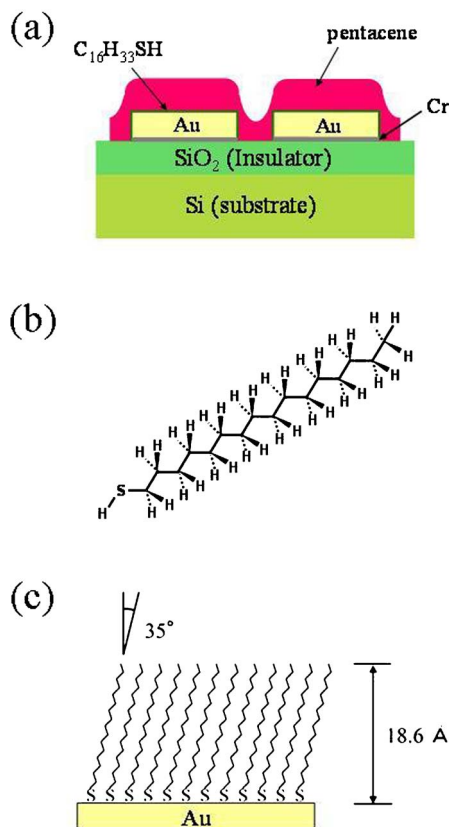


FIG. 1. (Color online) (a) Device structure of pentacene thin-film FET. The thicknesses of Cr, Au, and pentacene are 5, 50, and 50 nm, respectively. The channel width W and length L are 4000 and 30 μm , respectively. The thickness and capacitance C_0 of SiO_2 are 400 nm and $8.63 \times 10^{-9} \text{ F cm}^{-2}$, respectively. (b) Molecular structures of $C_{16}H_{33}SH$. (c) Schematic representation of the surface of Au electrodes modified by $C_{16}H_{33}SH$.

^{a)}Electronic mail: kubozono@cc.okayama-u.ac.jp

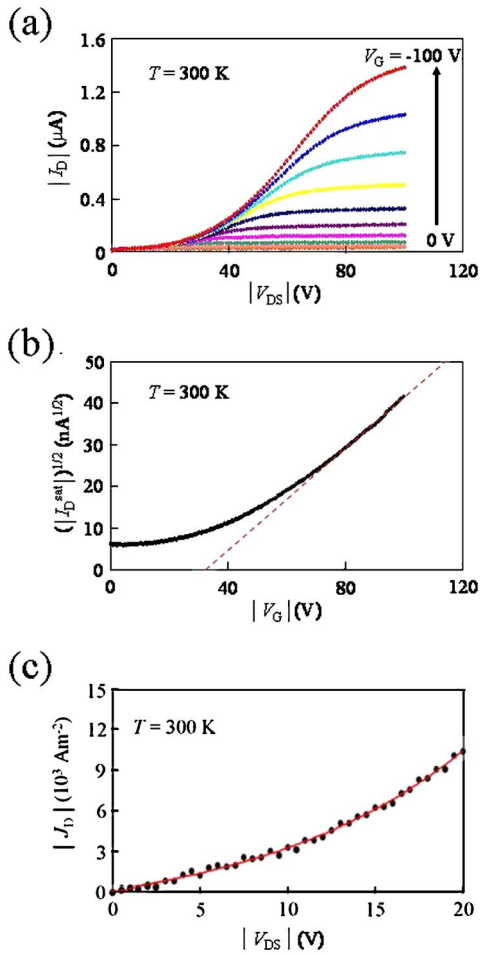


FIG. 2. (Color online) (a) $|I_D|$ - $|V_{DS}|$, (b) $|I_D^{\text{sat}}|^{1/2}$ - $|V_G|$, and (c) $|I_D|$ - $|V_{DS}|$ plots of pentacene/ $C_{16}H_{33}SH$ FET at 300 K. The fitted lines are drawn for (b) with $(|I_D^{\text{sat}}|)^{1/2} = (\mu WC_0/2L)^{1/2}(|V_G| - |V_T|)$ and for (c) with Eq. (3).

The absolute drain current $|I_D|$ versus absolute source-drain voltage $|V_{DS}|$ plots of the pentacene/ $C_{16}H_{33}SH$ FET device show p -channel normally off FET properties [Fig. 2(a)]. The $|I_D|$ - $|V_{DS}|$ plots also show clear concave-up non-linear behaviors in the low V_{DS} region, which shows that the hole transport is strongly suppressed by the large effective hole-injection barrier $\phi_{\text{bh}}^{\text{eff}}$. The $|I_D|$ increases linearly in the intermediate region for the pentacene/ $C_{16}H_{33}SH$ FET [Fig. 2(a)] and saturates in the high V_{DS} region.

The values of μ and V_T were determined from the drain current $|I_D^{\text{sat}}|$ in the saturation region ($V_{DS}=100$ V), i.e., $|I_D^{\text{sat}}|^{1/2}$ versus absolute gate voltage $|V_G|$ plot [Fig. 2(b)], to be $6.8 \times 10^{-4} \text{ cm}^2 \text{ V}^{-1} \text{ s}^{-1}$ and 35 V at 300 K, respectively. The μ value is lower by one order of magnitude than the value, $5.9 \times 10^{-3} \text{ cm}^2 \text{ V}^{-1} \text{ s}^{-1}$, of $C_{60}/C_{16}H_{33}SH$ FET.⁵ The absolute drain current density $|J_D|$ vs $|V_{DS}|$ plot in the low V_{DS} region (0–20 V) at $V_G=100$ V for the pentacene/ $C_{16}H_{33}SH$ FET device ($T=300$ K) is shown in Fig. 2(c) together with the calculated (fitting) line. The fitting line was drawn according to Eq. (1) based on the thermionic emission model expanded to double Schottky barriers because this device possesses two Au-pentacene junctions modified by $C_{16}H_{33}SH$ (source Au electrode-pentacene and pentacene-drain Au electrode),⁵

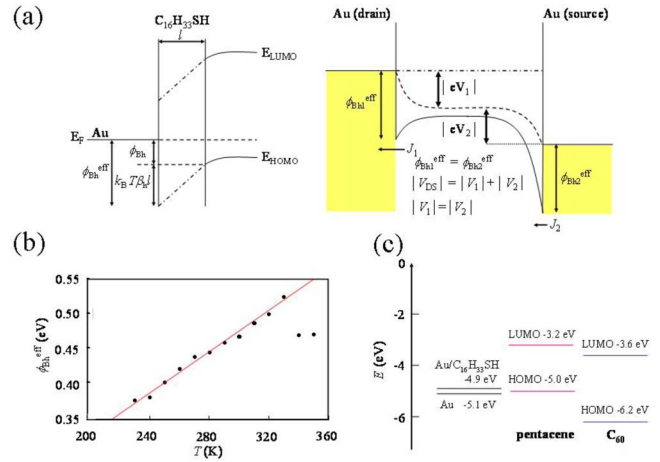


FIG. 3. (Color online) (a) (Left) Schematic representation of band bending for pentacene-Au junction modified by $C_{16}H_{33}SH$ and (right) that of band bending (solid line) for double Schottky barriers in pentacene/ $C_{16}H_{33}SH$ FET. In the right figure, the additional tunneling barriers due to $C_{16}H_{33}SH$ are not drawn. (b) $\phi_{\text{bh}}^{\text{eff}}$ - T plot for pentacene $C_{16}H_{33}SH$ /FET. (c) Band diagram of E_F of Au, E_{HOMO} , and E_{LUMO} of pentacene and C_{60} .

$$J_D = A^* T^2 \times \exp(-\phi_{\text{bh}}^{\text{eff}}/k_B T) \sinh[eV_{DS}/(2k_B T)] / \cosh(eV_{DS}/2k_B T), \quad (1)$$

where A^* , e , and k_B are the effective Richardson constant, electron charge, and Boltzmann constant, respectively. The A^* and $\phi_{\text{bh}}^{\text{eff}}$ are given by Eqs. (2) and (3), respectively,

$$A^* = 4\pi e m_p^* k_B^2 / h^3 \quad (2)$$

and

$$\phi_{\text{bh}}^{\text{eff}} = \phi_{\text{bh}} + k_B T \beta_h l. \quad (3)$$

Here m_p^* , h , ϕ_{bh} , β_h , and l are the effective mass of hole, Planck's constant, hole-injection barrier height of pure Au-pentacene junction, tunneling efficiency of hole, and length of tunneling barrier, respectively. In the analyses, the m_p^* was fixed to be $1.55m_0$ based on the value reported previously;⁹ m_0 is the electron rest mass. The term $k_B T \beta_h l$ in Eq. (3) refers to the additional tunneling barrier produced by insertion of $C_{16}H_{33}SH$.

The energy band diagram for the Au-pentacene junction modified by $C_{16}H_{33}SH$ and the simplified energy diagram for two junctions under the application of V_{DS} is shown in Fig. 3(a). In this model, most of V_{DS} is assumed to be applied to the interfaces of the two junctions because the channel resistance is small at $V_G=100$ V ($>V_T$ of 35 V) in comparison with the contact resistance. In the estimation of J_D , the thickness of channels is assumed to be 1 nm based on Ref. 10. The $\phi_{\text{bh}}^{\text{eff}}$ value at 300 K was determined to be 0.467 ± 0.003 eV by least-squares fitting to the J_D - V_{DS} plot (0–20 V) with Eq. (1). The n value at 300 K was 1.0043 ± 0.0002 . This value is close to the ideal value of unity, suggesting that two junctions of this device are almost ideal Schottky diodes. The $\phi_{\text{bh}}^{\text{eff}}$ value is smaller than the ϕ_B^{eff} ($=0.51 \pm 0.02$ eV) determined for the $C_{60}/C_{16}H_{33}SH$ FET.^{5,6}

In the $|I_D|$ - $|V_{DS}|$ plots ($V_G=100$ V) at 230–350 K for pentacene/ $C_{16}H_{33}SH$ FET, the large concave-up nonlinearity in the low V_{DS} region is observed in the plots at low T region (not shown). The $\phi_{\text{bh}}^{\text{eff}}$ value was determined from the J_D - V_{DS} plot of $V_{DS}=0$ –20 V at V_G of 100 V at each T with Eq. (1).

The $\phi_{\text{bh}}^{\text{eff}}-T$ plot is shown in Fig. 3(b). As expected from Eq. (3), the linear relationship was observed in the $\phi_{\text{bh}}^{\text{eff}}-T$ plot below 340 K. The values at 340 and 350 K deviate from the line. This corresponds to the variation from concave-up non-linear $I_{\text{D}}-V_{\text{DS}}$ curve to linear line above 330 K, which suggests that the hole-injection barrier is gradually destroyed because of the thermal fluctuation of $\text{C}_{16}\text{H}_{33}\text{SH}$ on Au electrodes.

The ϕ_{bh} and β_h values for pentacene/ $\text{C}_{16}\text{H}_{33}\text{SH}$ FET have been determined by least-squares fit to $\phi_{\text{bh}}^{\text{eff}}-T$ plot [Fig. 3(b)] with Eq. (3). When the l , 18.6 Å, of $\text{C}_{16}\text{H}_{33}\text{S}-\text{Au}$ is used as the length to the tunneling barrier in this analysis [Figs. 1(c) and 3(a)],⁸ the β_h value can be determined to be $0.91 \pm 0.03 \text{ \AA}^{-1}$, whose value is almost the same as the β value, $1.12 \pm 0.06 \text{ \AA}^{-1}$, for electron in $\text{C}_{60}/\text{C}_{16}\text{H}_{33}\text{SH}$ FET.^{5,6} This implies that the efficiency of the carrier tunneling across the CH_2 chain is not much different for electrons and holes. If a vacuum barrier was assumed between Au and pentacene, the β_h would be estimated to be 2.28 \AA^{-1} since the highest occupied molecular orbital (HOMO) level, E_{HOMO} , of pentacene and the E_{F} of Au modified by $\text{C}_{16}\text{H}_{33}\text{SH}$ is -5.0 and -4.9 eV, respectively, as seen from Fig. 3(c).^{1,5} This β_h value of 2.28 \AA^{-1} is more than two times larger than the experimental value ($0.91 \pm 0.03 \text{ \AA}^{-1}$). This result implies that the holes can pass through the $\text{C}_{16}\text{H}_{33}\text{S}-\text{Au}$ more easily than through the vacuum barrier.

The ϕ_{bh} value can be determined from the $\phi_{\text{bh}}^{\text{eff}}-T$ plot [Fig. 3(b)] to be 0.03 ± 0.01 eV. This value is smaller than that, 0.09 ± 0.03 eV, determined from the $\phi_b^{\text{eff}}-T$ plot for the $\text{C}_{60}/\text{C}_{16}\text{H}_{33}\text{SH}$ FET.⁵ From the band diagram of Au and pentacene, for holes, the Schottky barrier height between Au and pentacene can be expected to be 0.1 eV [Fig. 3(c)], whose value is slightly larger than the experimental ϕ_{bh} value of 0.03 ± 0.01 eV determined in this study. The deviation of experimental ϕ_{bh} from the value expected from the simple band picture may be due to the lowering of actual Schottky barrier height produced by interface states, mirror charge effect, and electric double layer formed at the interface. However, this deviation is much smaller than the case of $\text{Au}-\text{C}_{60}$ junctions

(experimental ϕ_B : 0.09 eV, the Schottky barrier height expected from simple band picture: 1.5 eV).⁵

In conclusion, the $J_{\text{D}}-V_{\text{DS}}$ curves of the pentacene/ $\text{C}_{16}\text{H}_{33}\text{SH}$ FET could be analyzed reasonably well within the thermionic emission model for double Schottky barriers, and the reliable values of ϕ_{bh} and β_h have been determined for the FET device. In the pentacene/ $\text{C}_{16}\text{H}_{33}\text{SH}$ FET device, more than 90% in the $\phi_{\text{bh}}^{\text{eff}}$ at 300 K is contributed from the additional tunneling barrier, which is associated with the tunneling of hole through $\text{C}_{16}\text{H}_{33}\text{SH}$ insulators inserted into the Au-pentacene junctions. As the reliable parameters for the Schottky barrier heights in the p -channel pentacene FET devices are obtained by the application of thermionic emission model for double Schottky barriers to the $J_{\text{D}}-V_{\text{DS}}$ curves in the same manner as the case of n -channel C_{60} FET,^{5,6} this analysis has been shown to be useful for the investigation of carrier injections in both n - and p -channel organic FET devices.

This study was partly supported by a Grant-in-Aid (18340104) from MEXT, Japan.

¹T. Yasuda, T. Goto, K. Fujita, and T. Tsutsui, Appl. Phys. Lett. **85**, 2098 (2004).

²T. Nishikawa, S. Kobayashi, T. Nakanowatari, T. Mitani, T. Shimoda, Y. Kubozono, G. Yamamoto, H. Ishii, M. Niwano, and Y. Iwasa, J. Appl. Phys. **97**, 104509 (2005).

³Y. Takahashi, T. Hasegawa, Y. Abe, Y. Tokura, and G. Saito, Appl. Phys. Lett. **88**, 073504 (2006).

⁴K. Ochi, T. Nagano, T. Ohta, R. Nouchi, Y. Kubozono, Y. Matsuoka, E. Shikoh, and A. Fujiwara, Appl. Phys. Lett. **89**, 083511 (2006).

⁵T. Nagano, M. Tsutsui, R. Nouchi, N. Kawasaki, Y. Ohta, Y. Kubozono, and N. Takahashi, A. Fujiwara, J. Phys. Chem. C. **111**, 7211 (2007).

⁶Y. Ohta, N. Kawasaki, T. Nagano, R. Nouchi, Y. Kubozono, and A. Fujiwara (unpublished).

⁷C. Schönberger, J. Jorritsma, J. A. M. Sondag-Huethorst, and L. G. J. Fokkink, J. Phys. Chem. **99**, 3259 (1995).

⁸D. M. Alloway, M. Hofmann, D. L. Smith, N. E. Gruhn, A. L. Graham, R. Colorado Jr., V. H. Wysocki, T. R. Lee, P. A. Lee, and N. R. Armstrong, J. Phys. Chem. B **107**, 11690 (2003).

⁹M. Nakamura, Abstract of IMR Symposium of Tohoku University, 2007 (unpublished), p. 10.

¹⁰T. Miyadera, M. Nakayama, and K. Saiki, Appl. Phys. Lett. **89**, 172117 (2006).